

Global Constraint Model for Microbial Growth Law

Jumpei F. Yamagishi^{1,2,*} and Tetsuhiro S. Hatakeyama^{3,2,†}

¹Center for Biosystems Dynamics Research, RIKEN, 6-2-3 Furuedai, Suita 565-0874, Japan

²Universal Biology Institute, The University of Tokyo, 7-3-1 Hongo, Tokyo 113-0033, Japan

³Earth-Life Science Institute, Tokyo Institute of Technology, Tokyo 152-8550, Japan

Monod’s law is a widely accepted phenomenology for bacterial growth. Since it has the same functional form as the Michaelis–Menten equation for enzyme kinetics, cell growth is often considered to be locally constrained by a single reaction. In contrast, this paper shows that a global constraint model of resource allocation to metabolic processes can well describe the nature of cell growth. This concept is a generalization of Liebig’s law, a growth law for higher organisms, and explains the dependence of microbial growth on the availability of multiple nutrients, in contrast to Monod’s law.

To understand complex living systems, universal phenomenological laws independent of specific species or molecules are of paramount importance [1]. In particular, the dependence of cellular growth rates on environmental conditions (and cellular physiological states) has been an important problem in biology for over a century [2–5]. The classical phenomenology, originally proposed by Monod in the 1940s [2], states that microbial growth kinetics, namely the dependence of the specific growth rate μ on substrate availability, generally follows the Monod equation:

$$\mu([S]) = \mu_{\max} \frac{[S]}{K_S + [S]}, \quad (1)$$

where μ_{\max} is the maximum growth rate and $[S]$ is the environmental concentration of the growth-limiting substrate S with its half-saturation concentration K_S .

Such behavior has often been attributed to a specific molecular biological process. Since the Monod equation (1) has the same functional form as the Michaelis–Menten equation, a single biochemical process is usually expected to limit cell growth [6–8] (see also Fig. 1a). In previous hypotheses, this single “black box” could be the substrate transport into cells [6, 9], the net flux of respiration [10], or the (coarse-grained) reaction that couples catabolism and anabolism [11].

However, microbial growth is achieved collectively by the interplay of thousands of biochemical processes. There is considerable experimental evidence that cell growth is not limited by a single biochemical process alone [12, 13]: for example, experimental changes in the environmental conditions of nitrogen sources can alter the dependence of growth rate on the availability of carbon sources [14, 15]; and cells exhibit qualitatively different phenotypes with respect to the metabolism of nutrients for cell growth [16].

In addition, the accumulation of experimental data has shown that the experimentally-observed microbial growth kinetics are not accurately captured by the Monod equation (1) [5, 6, 17, 18]. That is, the shape of actual microbial growth kinetics curves varies across species and environments and there is no longer quantitative evidence to support the ex-

act functional form of Eq. (1). Nevertheless, certain characteristics still appear to be universal: (i) growth rate is a monotonically increasing function of nutrient availability and (ii) growth rate exhibits concavity with respect to nutrient availability [19], in other words, there are diminishing returns to getting more and more of a nutrient.

Therefore, a novel macroscopic framework is essential to elucidate the general mechanism underlying these fundamental characteristics (i-ii) of the microbial growth kinetics curve. Based on the optimality principle of evolved metabolic systems, we show that the cellular growth rate gradually plateaus with increasing nutrient availability. This is because as the availability of a specific nutrient increases, some other resources are gradually depleted and thus act as additional growth-limiting factors (Fig. 1b). This framework can be seen as a generalized formulation of Liebig’s law of the minimum, a classical phenomenological theory of plant growth, which states that the availability of multiple resources collectively limits the growth of organisms [3, 15, 20] (see also Fig. 1c). It also provides new insights into the dependence of microbial growth rate on the environmental availability of multiple nutrient sources, which cannot be captured by Monod’s classical phenomenology.

Global constraint model of cell growth.— Cell growth requires the production of biomass through metabolism. We therefore focus on how the intracellular allocation of diverse resources to metabolic processes is globally constrained by stoichiometry and the law of matter conservation.

Let us denote all the intracellular metabolites and metabolic reactions as \mathcal{M} and \mathcal{R} , respectively. Here, by decomposing each reversible reaction into two irreversible reactions (i.e., its forward and backward components), a non-negative vector $\mathbf{v} := \{v_i\}_{i \in \mathcal{R}}$ represents the fluxes of all $|\mathcal{R}|$ reactions. Among $|\mathcal{M}|$ metabolites, the set of exchangeable metabolites is denoted by $\mathcal{E} (\subset \mathcal{M})$.

In the context of systems biology, the metabolic systems of cells are assumed to maximize their growth rate, or the biomass synthesis rate, as a natural consequence of evolution [16, 21–23]. Since we are considering continuously growing microbes, stationarity of intracellular concentrations of non-exchangeable metabolites $m (\in \mathcal{M} \setminus \mathcal{E})$ is also assumed. Then, the metabolic regulation of reaction fluxes \mathbf{v} can generally be formulated as a linear programming (LP) problem, as known as constraint-based modeling (CBM) of

* jumpei.yamagishi@riken.jp

† hatakeyama@elsi.jp

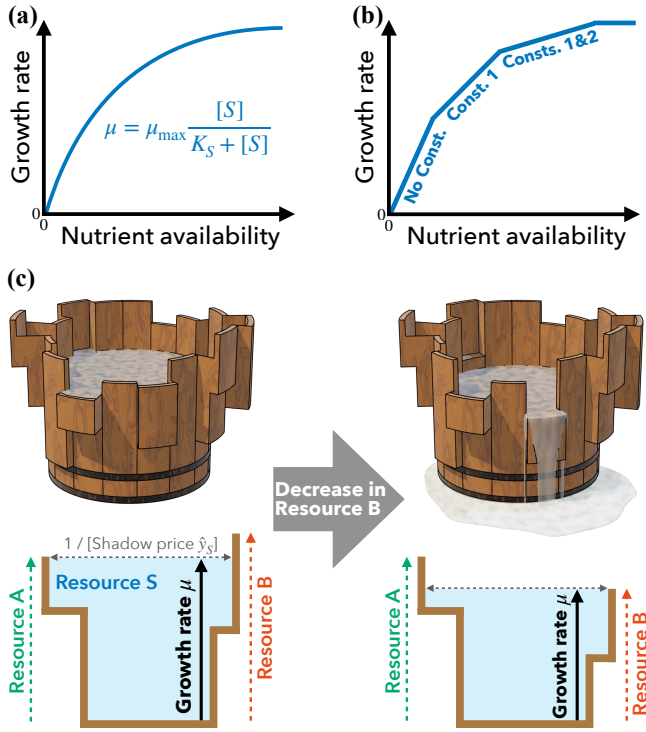


FIG. 1. Microbial growth kinetics. (a) Monod's microbial growth model. (b) Global constraint model for the microbial growth kinetics curve. (c) Terraced Liebig's barrel (top) and its sectional view for the case with a focal substrate S and the other resources A and B (bottom). As S is poured into the barrel, the surface height corresponds to the growth rate μ , while the height of each stave represents the availability of each nutrient or resource other than S . Each stave spreads out in a stepwise manner, reflecting the metabolic shifts to pathways with lower growth yield from S due to additional global constraints. (left) The shortest stave corresponds to resource A , which has the lowest availability, and thus it determines the maximum growth rate. (right) Due to a decrease in the availability of resource B , the maximum growth rate is limited by B . At the same time, the reallocation of B to metabolic processes and the resulting decrease in the shadow price \hat{y}_S (i.e., the slope of the growth kinetics curve) occur at lower availability of S .

metabolism [16, 24, 25]:

$$\max_{\mathbf{v} \geq 0} v_{\text{gr}} \quad \text{s.t.} \quad \sum_{i \in \mathcal{R}} S_{mi} v_i = 0 \quad (m \in \mathcal{M} \setminus \mathcal{E}), \quad (2)$$

$$\sum_{i \in \mathcal{R}} S_{mi} v_i + I_m \geq 0 \quad (m \in \mathcal{E}), \quad (3)$$

$$\sum_{i \in \mathcal{R}} C_{ai} v_i \leq I_a \quad (a \in \mathcal{C}), \quad (4)$$

where $\text{gr} (\in \mathcal{R})$ denotes the growth or biomass synthesis reaction. S_{mi} is the stoichiometric coefficient representing that metabolic reaction $i (\in \mathcal{R})$ produces (consumes) $|S_{mi}|$ molecules of metabolite $m (\in \mathcal{M})$ if $S_{mi} > 0$ (if $S_{mi} < 0$). $\sum_i S_{mi} v_i$ is then the excess production of metabolite m . Thus, equalities (2) represent that the production and degradation of internal metabolites must be balanced, and inequalities (3) represent that exchangeable metabolites m with

maximum influx $I_m > 0$ (efflux $I_m < 0$) are taken up (degraded). Finally, the other constraints on the allocation of the non-nutrient resources \mathcal{C} such as the total amount of enzymes [26, 27], membrane surface [28], and Gibbs energy dissipation [29] can be incorporated as inequalities (4). Supplemental Material (SM), Table S1 collects all the notation in one place.

The solution to the LP problem (2-4) is denoted as $\hat{\mathbf{v}}(\mathbf{I})$; since the optimal objective function $\hat{v}_{\text{gr}}(\mathbf{I})$ is the predicted value of the growth rate $\mu(\mathbf{I})$, we will hereafter refer to $\hat{v}_{\text{gr}}(\mathbf{I})$ as $\mu(\mathbf{I})$. Numerical calculations of the CBM method successfully explain and predict experimental data, at least for model organisms such as *E. coli* strains [16, 21, 22, 30].

Monotonicity and concavity of growth kinetics curve.— The calculated growth rate satisfies fundamental characteristics (i-ii) of the microbial growth kinetics curve. Here we show that the dependence of the growth rate μ on the maximum influx I_S of a given nutrient $S (\in \mathcal{E})$ is generally a monotonically increasing and concave function. While such properties have sometimes been recognized empirically for specific metabolic models and parameters [31, 32], its generality can be proven mathematically as follows.

First, the monotonic increase in the growth kinetics curve $\mu(I_S; \tilde{\mathbf{I}})$, where $\tilde{\mathbf{I}} := \{I_a\}_{a \in \mathcal{E} \cup \mathcal{C} \setminus \{S\}}$ denotes the availability of the resources other than the nutrient S , is evident because increasing the maximum nutrient influx from I_S to $I_S + \Delta I_S$ expands the feasible solution space of the LP problem (2-4).

To prove the concavity of the growth kinetics curve $\mu(I_S; \tilde{\mathbf{I}})$, it suffices to show that its slope, $\partial \mu / \partial I_S$, monotonically decreases as I_S increases. Remarkably, the slope coincides with the so-called shadow price \hat{y}_S of nutrient S [33–35], where \hat{y} denotes the solution to the dual problem defined below and its element \hat{y}_a quantifies the growth return to the additional consumption of resource $a (\in \mathcal{E} \cup \mathcal{C})$. In the following, we show that shadow price $\hat{y}_S(I_S; \tilde{\mathbf{I}})$ diminishes monotonically with I_S .

The dual problem to the primal LP problem (2-4) is given as [24, 33, 36] (see also SM, Appendix A for the derivation):

$$\min_{\mathbf{y} \in \mathbb{R}^{\mathcal{M} \cup \mathcal{C}}} \sum_{a \in \mathcal{E} \cup \mathcal{C}} I_a y_a \quad \text{s.t.} \quad (-S^\top \quad C^\top) \mathbf{y} \geq \mathbf{1}_{\text{gr}}, \quad (5)$$

$$y_a \geq 0 \quad (a \in \mathcal{E} \cup \mathcal{C}).$$

Here $\mathbf{1}_{\text{gr}}$ denotes a $|\mathcal{R}|$ -dimensional vector, where the gr -th element is one and all other elements are zero. From the duality theorem [36], the maximized objective function of the primal problem (2-4) is equal to the minimized objective function of the dual problem (5): i.e., $\mu(\mathbf{I}) = \sum_a I_a \hat{y}_a(\mathbf{I})$. The optimal solution $\hat{\mathbf{y}}$ to the dual problem thus satisfies $\hat{y}_a = \partial \mu / \partial I_a$ for arbitrary $a (\in \mathcal{E} \cup \mathcal{C})$. To prove the monotonicity of $\hat{y}_S(I_S; \tilde{\mathbf{I}})$, let us define a vector \mathbf{I}' which differs from the vector \mathbf{I} only in the S -th element: i.e., $I'_S = I_S + \Delta I_S$ and $I'_m = I_m$ for $m (\neq S)$. From the definition, the solutions of the minimization problem (5) with the parameters \mathbf{I} and \mathbf{I}' , $\hat{\mathbf{y}}(\mathbf{I})$ and $\hat{\mathbf{y}}(\mathbf{I}')$,

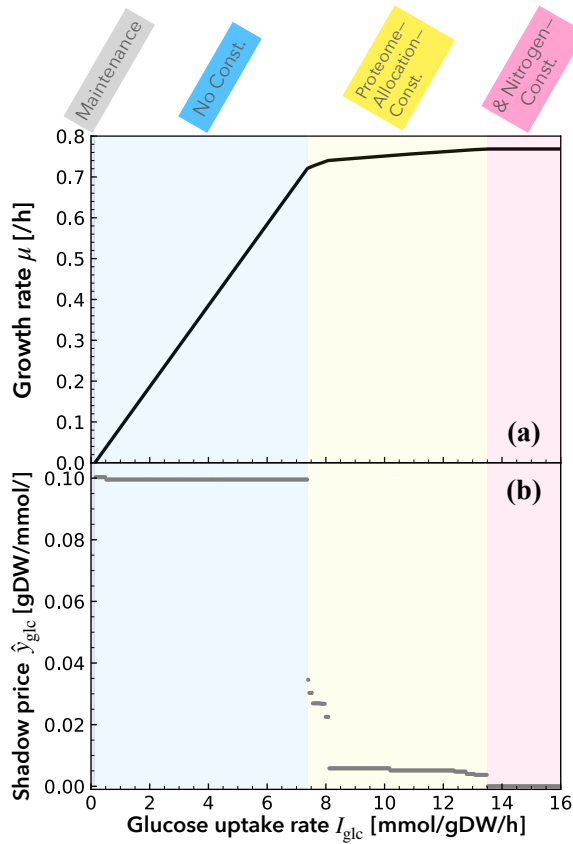


FIG. 2. (a) Growth rate μ and (b) shadow price \hat{y}_{glc} of glucose as a function of carbon source availability I_{glc} with $I_{\text{amm}} = 8.3$. Numerical calculations of a CBM method, constrained allocation flux balance analysis (CAFBA) [27], were performed using the genome-scale *E.coli* iJO1366 model [38] and the COBRApy package [39].

satisfy $\mathbf{I} \cdot \hat{\mathbf{y}}(\mathbf{I}') \geq \mathbf{I} \cdot \hat{\mathbf{y}}(\mathbf{I})$ and $\mathbf{I}' \cdot \hat{\mathbf{y}}(\mathbf{I}) \geq \mathbf{I}' \cdot \hat{\mathbf{y}}(\mathbf{I}')$. It follows

$$\begin{aligned} \mathbf{I} \cdot \hat{\mathbf{y}}(\mathbf{I}') + \mathbf{I}' \cdot \hat{\mathbf{y}}(\mathbf{I}) &\geq \mathbf{I} \cdot \hat{\mathbf{y}}(\mathbf{I}) + \mathbf{I}' \cdot \hat{\mathbf{y}}(\mathbf{I}') \\ \Leftrightarrow (\mathbf{I}' - \mathbf{I}) \cdot [\hat{\mathbf{y}}(\mathbf{I}') - \hat{\mathbf{y}}(\mathbf{I})] &\leq 0 \\ \Leftrightarrow \Delta I_S [\hat{y}_S(\mathbf{I}') - \hat{y}_S(\mathbf{I})] &\leq 0 \\ \Leftrightarrow \frac{\hat{y}_S(I_S + \Delta I_S; \tilde{\mathbf{I}}) - \hat{y}_S(I_S; \tilde{\mathbf{I}})}{\Delta I_S} &\leq 0. \end{aligned}$$

The duality also allows us to prove the concavity of $\mu(\mathbf{I})$ as a multivariable function of \mathbf{I} (SM, Appendix B).

It is thus concluded that the monotonicity and concavity of the microbial growth kinetics curve, fundamental characteristics (i-ii), are universal for LP problems including CBM [37].

To confirm the above analytical results, we also performed numerical simulations of CBM with a genome-scale metabolic network of *E.coli* [38]. The resulting piecewise linear growth kinetics curve $\mu(I_{\text{glc}})$ is indeed monotonically increasing and concave (Fig. 2a), as its slope $\hat{y}_{\text{glc}} = \partial\mu/\partial I_{\text{glc}}$ monotonically decreases to zero (Fig. 2b).

Each locally linear part of the microbial growth kinetics curve represents a distinct phenotype phase, i.e., a qualitatively different metabolic phenotype with a different combination of growth-limiting constraints [35]. In the case of Fig. 2,

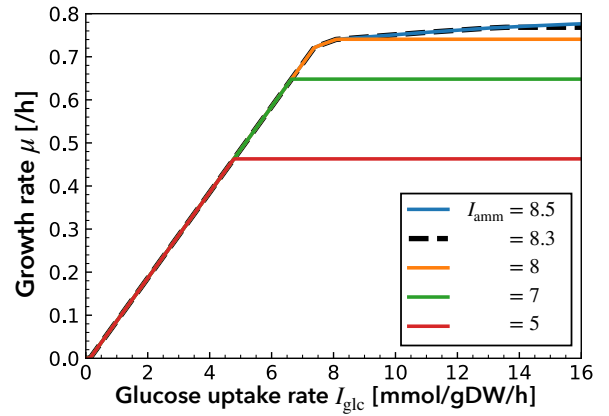


FIG. 3. Growth rate μ as a function of carbon source availability I_{glc} with different nitrogen source availability I_{amm} .

in the blue region with small I_{glc} , only carbon source intake is the growth-limiting factor [40]. Due to the limited amount of protein, carbon metabolism at intermediate I_{glc} (the yellow region) reallocates enzymes to less efficient metabolic reactions in terms of growth yield, which gradually diminishes the growth return to additional glucose intake. Finally, in the red region, the intake of the nitrogen source (ammonium) determines the maximum growth rate. A

Growth rate dependence on multiple nutrients.— The global constraint model not only reproduces the known fundamental characteristics (i-ii) of the microbial growth kinetics curve, but also serves as a phenomenological theory for the dependence of growth rate on multiple nutrients. The dependence of the growth rate on the availability of non-substitutable nutrient sources (e.g., carbon and nitrogen sources) can be calculated numerically, and the calculated $\mu(\mathbf{I})$ is monotonically increasing and concave with respect to \mathbf{I} (see SM, Appendix B).

Since the growth kinetics curve $\mu(I_S; \tilde{\mathbf{I}})$ is shaped by the global regulation of intracellular metabolism, it depends not only on the availability of the focal nutrient S but also on that of the other resources, here denoted as $\tilde{\mathbf{I}}$. If the intake I_m of metabolite m ($m \neq S$) increases (decreases), the constraint on the allocation of metabolite m is relaxed (tightened); as a result, the growth kinetics curve $\mu(I_S; \tilde{\mathbf{I}})$ should shift up (down) in the phase(s) where cell growth is limited by metabolite m (see also Fig. 1c). Conversely, by measuring how the shape of the microbial growth kinetics curve responds to environmental manipulations, such as the addition of a nutrient to the medium, one can empirically infer the growth-limiting factors under the original environmental conditions.

Such responses of the microbial growth kinetics curve are indeed observed numerically (Fig. 3). In this case, the increase (decrease) in ammonium influx I_{amm} shifts the growth kinetics curve up (down) in the phase with sufficiently large I_{glc} (shown in red in Fig. 2). From this observation, one can empirically conclude that cell growth in this phase is limited by the nitrogen source under the original environment of $I_{\text{amm}} = 8.3$, without further information from the numerical

experiments.

In this paper, we have shown that the fundamental characteristics of the microbial growth kinetics curve can be explained as general properties of optimal resource allocation in cellular metabolism: as the availability of a nutrient increases, its metabolism into biomass becomes constrained by the intracellular allocation of other resources, which gradually diminishes the growth return to the additional intake of the nutrient (see also Fig. 1bc). Such a perspective was originally established in previous research on the microeconomic formulation of cellular metabolism [25, 32], and it has been refined into a general formalism. Note that microbial growth kinetics curves are often naively assumed to be smooth functions in the form of the Monod equation (1); however, apparently multiphasic growth kinetics curves, which are non-smooth at the boundaries between different phenotype phases, have been observed experimentally [29, 41]. The global constraint model can describe the microbial growth kinetics curve with arbitrary precision, at least if a sufficient number of constraints are considered.

The global constraint model for microbial growth kinetics also provides a theoretical basis for the dependence of growth rate on the availability of multiple nutrient sources, which cannot be captured by the classical arguments about Monod's bacterial growth model. In particular, we elucidated how the microbial growth kinetics curve $\mu(I_S)$ responds to manipulating the environmental availability of a nutrient other than the focal nutrient S . Remarkably, this model can be viewed as a generalized formulation of Liebig's law of the minimum,

which states that the growth rate of an organism is determined by the availability of the scarcest resource. Liebig's law is commonly illustrated by the metaphor of a barrel with uneven staves [42], as the feasible water surface height of the barrel is limited by the shortest staff. This barrel metaphor describes the effect of resource availability on the maximum growth rate, but does not account for growth kinetics. In contrast, the global constraint model, which incorporates the influence of resource allocation on growth kinetics, is also illustrated schematically using a modified Liebig's barrel with terraced staves (Fig. 1c): at the water level where an additional global constraint appears, each staff of the terraced Liebig's barrel spreads out in a stepwise manner, making further increases in growth rate more difficult.

The present study revisited the classical phenomenological laws in biology, Monod's law of bacterial growth and Liebig's law of the minimum, from the perspective of resource allocation in cellular metabolism. We thereby provided a comprehensive theory of the relationship between microbial growth and nutrient availability. As Liebig's law was originally formulated to describe the growth of plants, we expect our theory to provide a theoretical basis for the growth of higher organisms as well as microbes in the future.

We would like to thank Takuma Ōnishi for his assistance in the preparation of Fig. 1c. J. F. Y. is supported by the RIKEN Research Fund for Special Postdoctoral Researcher (project code: 202401061031) and the Masason Foundation. T. S. H. is supported by JSPS KAKENHI Grant Number JP21K15048.

-
- [1] K. Kaneko, *Life: an introduction to complex systems biology* (Springer, 2006).
- [2] J. Monod, "The growth of bacterial cultures," *Annual review of microbiology* **3**, 371–394 (1949).
- [3] A. R. Whitson and H. L. Walster, *Soils and soil fertility* (Webb Publishing Company, 1912).
- [4] M. Scott and T. Hwa, "Bacterial growth laws and their applications," *Current Opinion in Biotechnology* **22**, 559–565 (2011).
- [5] K. Kovárová-Kovar and T. Egli, "Growth kinetics of suspended microbial cells: from single-substrate-controlled growth to mixed-substrate kinetics," *Microbiology and Molecular Biology Reviews* **62**, 646–666 (1998).
- [6] J. G. Reich and E. Selkov, *Energy metabolism of the cell: a theoretical treatise* (Academic Press, 1981).
- [7] D. Sher, D. Segrè, and M. J. Follows, "Quantitative principles of microbial metabolism shared across scales," *Nature Microbiology*, 1–14 (2024).
- [8] Y. Liu, "Overview of some theoretical approaches for derivation of the monod equation," *Applied microbiology and biotechnology* **73**, 1241–1250 (2007).
- [9] J. C. Merchuk and J. A. Asenjo, "The monod equation and mass transfer," *Biotechnology and Bioengineering* **45**, 91–94 (1995).
- [10] Q. Jin and C. M. Bethke, "A new rate law describing microbial respiration," *Applied and Environmental Microbiology* **69**, 2340–2348 (2003).
- [11] J. J. Heijnen and B. Romein, "Derivation of kinetic equations for growth on single substrates based on general properties of a simple metabolic network," *Biotechnology Progress* **11**, 712–716 (1995).
- [12] A. L. Koch, "Microbial physiology and ecology of slow growth," *Microbiology and Molecular Biology Reviews* **61**, 305–318 (1997).
- [13] A. Goelzer and V. Fromion, "Bacterial growth rate reflects a bottleneck in resource allocation," *Biochimica et Biophysica Acta (BBA)-General Subjects* **1810**, 978–988 (2011).
- [14] A. Bren, J. O. Park, B. D. Towbin, E. Dekel, J. D. Rabinowitz, and U. Alon, "Glucose becomes one of the worst carbon sources for e. coli on poor nitrogen sources due to suboptimal levels of cAMP," *Scientific Reports* **6**, 24834 (2016).
- [15] J. Tang and W. J. Riley, "Finding liebig's law of the minimum," *Ecological Applications* **31**, e02458 (2021).
- [16] B. Ø. Palsson, *Systems Biology: Constraint-based Reconstruction and Analysis* (Cambridge University Press, 2015).
- [17] U. Sommer, "A comparison of the droop and the monod models of nutrient limited growth applied to natural populations of phytoplankton," *Functional Ecology*, 535–544 (1991).
- [18] H. Wang, P. V. Garcia, S. Ahmed, and C. M. Heggerud, "Mathematical comparison and empirical review of the monod and droop forms for resource-based population dynamics," *Ecological Modelling* **466**, 109887 (2022).
- [19] Empirically, there can be a finite minimum substrate concentration $[S]_{\min}$ to achieve cell growth due to the maintenance energy requirements [5, 13]. However, in classical arguments such as Monod's, they are effectively ignored for simplicity by considering the substrate concentration $[S]$ after subtracting $[S]_{\min}$.

- [20] J. von Liebig, *Organic chemistry in its applications to agriculture and physiology* (Taylor and Walton, 1840).
- [21] N. E. Lewis, H. Nagarajan, and B. Ø. Palsson, “Constraining the metabolic genotype–phenotype relationship using a phylogeny of in silico methods,” *Nature Reviews Microbiology* **10**, 291–305 (2012).
- [22] R. U. Ibarra, J. S. Edwards, and B. Ø. Palsson, “Escherichia coli k-12 undergoes adaptive evolution to achieve in silico predicted optimal growth,” *Nature* **420**, 186–189 (2002).
- [23] E. Klipp, W. Liebermeister, C. Wierling, and A. Kowald, *Systems Biology: a textbook* (John Wiley & Sons, New Jersey, 2016).
- [24] P. B. Warren and J. L. Jones, “Duality, thermodynamics, and the linear programming problem in constraint-based models of metabolism,” *Physical Review Letters* **99**, 108101 (2007).
- [25] J. F. Yamagishi and T. S. Hatakeyama, “Linear response theory of evolved metabolic systems,” *Physical Review Letters* **131**, 028401 (2023).
- [26] M. Basan, S. Hui, H. Okano, Z. Zhang, Y. Shen, J. R. Williamson, and T. Hwa, “Overflow metabolism in escherichia coli results from efficient proteome allocation,” *Nature* **528**, 99–104 (2015).
- [27] M. Mori, T. Hwa, O. C. Martin, A. De Martino, and E. Marinari, “Constrained allocation flux balance analysis,” *PLoS Computational Biology* **12**, e1004913 (2016).
- [28] M. Szenk, K. A. Dill, and A. M. R. de Graff, “Why do fast-growing bacteria enter overflow metabolism? testing the membrane real estate hypothesis,” *Cell Systems* **5**, 95–104 (2017).
- [29] B. Niebel, S. Leupold, and M. Heinemann, “An upper limit on gibbs energy dissipation governs cellular metabolism,” *Nature Metabolism* **1**, 125–132 (2019).
- [30] Y. Shinfuku, N. Sorpitiporn, M. Sono, C. Furusawa, T. Hirasawa, and H. Shimizu, “Development and experimental verification of a genome-scale metabolic model for corynebacterium glutamicum,” *Microbial Cell Factories* **8**, 1–15 (2009).
- [31] H. Zeng and A. Yang, “Bridging substrate intake kinetics and bacterial growth phenotypes with flux balance analysis incorporating proteome allocation,” *Scientific Reports* **10**, 4283 (2020).
- [32] J. F. Yamagishi and T. S. Hatakeyama, “Microeconomics of metabolism: the warburg effect as giffen behaviour,” *Bulletin of Mathematical Biology* **83**, 120 (2021).
- [33] E. Reznik, P. Mehta, and D. Segrè, “Flux imbalance analysis and the sensitivity of cellular growth to changes in metabolite pools,” *PLoS Computational Biology* **9**, e1003195 (2013).
- [34] A. Varma, B. W. Boesch, and B. Ø. Palsson, “Stoichiometric interpretation of escherichia coli glucose catabolism under various oxygenation rates,” *Applied and environmental microbiology* **59**, 2465–2473 (1993).
- [35] J. S. Edwards, R. Ramakrishna, and B. Ø. Palsson, “Characterizing the metabolic phenotype: a phenotype phase plane analysis,” *Biotechnology and Bioengineering* **77**, 27–36 (2002).
- [36] R. J. Vanderbei, “Linear programming: foundations and extensions,” *Journal of the Operational Research Society* **49**, 94–94 (1998).
- [37] Strictly speaking, the growth kinetics curve discussed in the context of Monod’s growth law is $\mu([S])$, which differs in its argument from the $\mu(I_S)$ obtained in the current argument: nutrient concentration $[S]$ and nutrient intake I_S are not exactly the same. However, in the case of a linear intake $I_S \propto [S]$, the monotonicity and concavity of the growth kinetics curve hold. Even in the case of nonlinear transport, as long as the intake function $I_S([S])$ satisfies the monotonicity and convexity conditions as in the Michaelis–Menten equation, the monotonicity and convexity of the growth kinetics curve are satisfied if we consider the composite function $\mu([S]) = \mu(I_S; \tilde{\mathbf{I}}) \circ I_S([S])$.
- [38] J. D. Orth, T. M. Conrad, J. Na, J. A. Lerman, H. Nam, A. M. Feist, and B. Ø. Palsson, “A comprehensive genome-scale reconstruction of escherichia coli metabolism—2011,” *Molecular Systems Biology* **7**, 535 (2011).
- [39] A. Ebrahim, J. A. Lerman, B. Ø. Palsson, and D. R. Hyduke, “Cobrapy: Constraints-based reconstruction and analysis for python,” *BMC Syst Biol* **7** (2013).
- [40] The gray region with almost zero I_{glc} corresponds to the case with no solution due to the non-growth-associated maintenance energy requirements [43]. It is consistent with the empirically observed minimum substrate concentration $[S]_{\text{min}}$ to achieve cell growth.
- [41] W. G. Sunda, K. W. Shertzer, and D. R. Hardison, “Ammonium uptake and growth models in marine diatoms: Monod and droop revisited,” *Marine Ecology Progress Series* **386**, 29–41 (2009).
- [42] A. R. Whitson and H. L. Walster, *Notes on Soils: An Outline for an Elementary Course in Soils* (The authors, 1909).
- [43] I. Thiele and B. Ø. Palsson, “A protocol for generating a high-quality genome-scale metabolic reconstruction,” *Nature Protocols* **5**, 93–121 (2010).

**Supplemental Material for Jumpei F. Yamagishi and Tetsuhiro S. Hatakeyama
“Global Constraint Model for Microbial Growth Law”**

TABLE S1. Notations in the main text

Symbol	Description
μ	Growth rate
$[S]$	Environmental concentration of (growth-limiting) nutrient S
\mathcal{M}, \mathcal{E}	Set of metabolites / exchangeable metabolites ($\mathcal{E} \subset \mathcal{M}$)
\mathcal{C}	Set of non-nutrient resources
\mathcal{R}	Set of reactions
gr	Growth or biomass synthesis reaction ($\text{gr} \in \mathcal{R}$)
S, C	Stoichiometry matrix ($S := \{S_{mi}\}_{m \in \mathcal{M}, i \in \mathcal{R}}$) and resource allocation matrix ($C := \{C_{ai}\}_{a \in \mathcal{C}, i \in \mathcal{R}}$)
I_a	Maximal intake of exchangeable metabolite a ($\in \mathcal{E}$) or total capacity for non-nutrient resource a ($\in \mathcal{C}$)
\mathbf{I}	Availability of the resources ($\mathbf{I} := \{I_a\}_{a \in \mathcal{E} \cup \mathcal{C}}$)
$\tilde{\mathbf{I}}$	Availability of the resources other than nutrient S ($\tilde{\mathbf{I}} := \{I_a\}_{a \in \mathcal{E} \cup \mathcal{C} \setminus \{S\}}$)
v_i	Non-negative flux of reaction i ($\in \mathcal{R}$)
$\mathbf{v}, \hat{\mathbf{v}}$	Reaction fluxes ($\mathbf{v} := \{v_i\}_{i \in \mathcal{R}}$) and its optimized solution ($\hat{\mathbf{v}} := \{\hat{v}_i\}_{i \in \mathcal{R}}$)
\hat{y}_a	Shadow price of metabolite a ($\in \mathcal{M}$) or non-nutrient resource a ($\in \mathcal{C}$)
$\mathbf{y}, \hat{\mathbf{y}}$	Variables of dual problem (5) ($\mathbf{y} := \{y_a\}_{a \in \mathcal{M} \cup \mathcal{C}}$) and its optimized solution (i.e., shadow prices $\hat{\mathbf{y}} := \{\hat{y}_a\}_{a \in \mathcal{M} \cup \mathcal{C}}$)

Appendix A: Derivation of the dual problem (5)

It is equivalent to the dual problem (5) in the main text.

To derive the dual problem, let us introduce matrices

$$\mathbf{N}^{\text{int}} := -S^{\mathcal{M} \setminus \mathcal{E}} = \{-S_{ai}\}_{a \in \mathcal{M} \setminus \mathcal{E}, i \in \mathcal{R}},$$

$$\mathbf{N}^{\text{ex}} := \begin{pmatrix} -S^{\mathcal{E}} \\ \mathbf{C} \end{pmatrix},$$

with $S^{\mathcal{E}} := \{S_{ai}\}_{a \in \mathcal{E}, i \in \mathcal{R}}$, and rewrite the linear programming (LP) problem (2-4) as

$$\max_{\mathbf{v}} v_{\text{gr}} \quad \text{s.t.} \quad \mathbf{N}^{\text{int}} \mathbf{v} = \mathbf{0}, \quad \mathbf{N}^{\text{ex}} \mathbf{v} \leq \mathbf{I}, \quad \mathbf{v} \geq \mathbf{0}.$$

Then, the dual problem to this primal LP program (2-4) is formally derived as

$$\min_{\mathbf{y} \in \mathbb{R}^{\mathcal{M} \cup \mathcal{C}}} \begin{pmatrix} \mathbf{0} \\ \mathbf{I} \end{pmatrix} \cdot \mathbf{y} \quad \text{s.t.} \quad \begin{pmatrix} \mathbf{N}^{\text{int} \top} & \mathbf{N}^{\text{ex} \top} \\ \mathbf{0} & \mathbf{I} \end{pmatrix} \mathbf{y} \geq \mathbf{1}_{\text{gr}},$$

where \mathbf{I} is the $(\mathcal{E} \cup \mathcal{C}) \times (\mathcal{E} \cup \mathcal{C})$ identity matrix and $\mathbf{1}_{\text{gr}} \in \{0, 1\}^{\mathcal{R} \cup \mathcal{E} \cup \mathcal{C}}$ denotes a vector where the gr-th element is unity and all other elements are zero [24, 33, 36]. This can be rewritten as

$$\begin{aligned} & \min_{\mathbf{y} \in \mathbb{R}^{\mathcal{M} \cup \mathcal{C}}} \sum_{a \in \mathcal{E} \cup \mathcal{C}} I_a y_a \\ & \text{s.t.} \quad - \sum_{m \in \mathcal{M}} S_{mi} y_m + \sum_{a \in \mathcal{C}} C_{ai} y_a \geq 0 \quad (i \in \mathcal{R} \setminus \{\text{gr}\}), \\ & \quad - \sum_{m \in \mathcal{M}} S_{m, \text{gr}} y_m + \sum_{a \in \mathcal{C}} C_{a, \text{gr}} y_a \geq 1, \\ & \quad y_a \geq 0 \quad (a \in \mathcal{E} \cup \mathcal{C}). \end{aligned}$$

Appendix B: Proof of the concavity of optimal objective function

The concavity of optimal objective function $\hat{v}_{\text{gr}}(\mathbf{I})$ as a multivariable function of \mathbf{I} can be analytically proven as follows.

From the LP duality theorem [36] and the dual problem (5),

$$\hat{v}_{\text{gr}}(\mathbf{I}) = \min_{\mathbf{y} \in \mathbb{R}^{\mathcal{M}_{\text{UC}}}} \{\mathbf{I} \cdot \mathbf{y}_{\mathcal{EUC}} \mid (-\mathbf{S}^\top \quad \mathbf{C}^\top) \mathbf{y} \geq \mathbf{1}_{\text{gr}}, \mathbf{y}_{\mathcal{EUC}} \geq \mathbf{0}\},$$

where $\mathbf{y}_{\mathcal{EUC}}$ is defined as $\mathbf{y}_{\mathcal{EUC}} := \{y_a\}_{a \in \mathcal{EUC}}$ and $\mathbf{1}_{\text{gr}} \in \{0, 1\}^{\mathcal{R}}$ denotes a vector where the gr-th element is unity and all other elements are zero. In contrast to the primal problem (2-4), it is useful that the feasible solution space of the dual problem (5) does not change when \mathbf{I} is varied.

Thus, for arbitrary $0 < t < 1$ and $\mathbf{I}_1, \mathbf{I}_2$,

$$\begin{aligned} & \hat{v}_{\text{gr}}(t\mathbf{I}_1 + (1-t)\mathbf{I}_2) \\ &= \min_{\mathbf{y}} \{(t\mathbf{I}_1 + (1-t)\mathbf{I}_2) \cdot \mathbf{y}_{\mathcal{EUC}} \mid (-\mathbf{S}^\top \quad \mathbf{C}^\top) \mathbf{y} \geq \mathbf{1}_{\text{gr}}, \mathbf{y}_{\mathcal{EUC}} \geq \mathbf{0}\} \\ &\geq \min_{\mathbf{y}} \{t\mathbf{I}_1 \cdot \mathbf{y}_{\mathcal{EUC}} \mid (-\mathbf{S}^\top \quad \mathbf{C}^\top) \mathbf{y} \geq \mathbf{1}_{\text{gr}}, \mathbf{y}_{\mathcal{EUC}} \geq \mathbf{0}\} \\ &\quad + \min_{\mathbf{y}} \{(1-t)\mathbf{I}_2 \cdot \mathbf{y}_{\mathcal{EUC}} \mid (-\mathbf{S}^\top \quad \mathbf{C}^\top) \mathbf{y} \geq \mathbf{1}_{\text{gr}}, \mathbf{y}_{\mathcal{EUC}} \geq \mathbf{0}\} \\ &= t\hat{v}_{\text{gr}}(\mathbf{I}_1) + (1-t)\hat{v}_{\text{gr}}(\mathbf{I}_2). \end{aligned}$$

This is the definition of the concavity.